

Synthesis, crystal structure and magnetic properties of two new dicyanamide bridged 2D and 1D complexes of Mn(II)

Sudipta Dalai,^a Partha Sarathi Mukherjee,^b Ennio Zangrando^{*c} and Nirmalendu Ray Chaudhuri^{*a}

^a Department of Inorganic Chemistry, Indian Association for the Cultivation of Science, Jadavpur, Kolkata 700 032, India. E-mail: icnrc@mahendra.iacs.res.in; Fax: +91 33 473 2805.

^b Department of Chemistry, Kalna College, Kalna, Burdwan 713 409, India

^c Dipartimento di Scienze Chimiche, University of Trieste, 34127, Trieste, Italy. E-mail: zangrando@univ.trieste.it

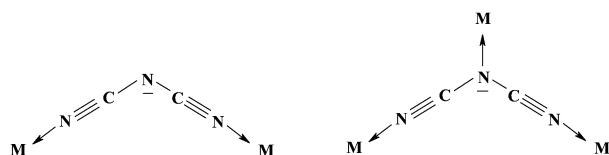
Received (in Montpellier, France) 5th March 2002, Accepted 14th May 2002

First published as an Advance Article on the web 16th August 2002

Two new polymeric compounds, $[\text{Mn}(\text{dca})_2(4\text{CN-py})_2]_n$ (**1**) and $[\text{Mn}(\text{dca})_2(\text{bpe})]_n$ (**2**) where dca = dicyanamide anion, 4CN-py = 4-cyanopyridine and bpe = 1,2-bis(4-pyridyl)ethane, have been synthesised and characterised by X-ray crystallography and low temperature magnetic study. Compound **1** consists of a two-dimensional network of octahedrally coordinated Mn(II) cations bridged by dicyanamide anions. In this compound, the Mn(II) cation is linked by four dca bridging ligands and two monodentate 4CN-py ligands. Compound **2** is an one-dimensional chain of Mn(II) bridged by dca as well as bpe. Each Mn(II) in the chain is octahedrally coordinated by four dca and two bpe ligands. Variable temperature magnetic susceptibility measurements in the temperature range 300–2 K reveal the existence of weak antiferromagnetic interactions in both complexes ($J = -0.154 \text{ cm}^{-1}$, $g = 2.01$ for **1** and $J = -1.25 \text{ cm}^{-1}$, $g = 2.00$ for **2**).

The study of multidimensional molecule-based magnetic materials is at the forefront of modern research.^{1–6} Use of dicyanamide (dca) as a bridging ligand to construct polynuclear systems is a continuous challenge due to the large variety of topologies and magnetic properties that may be obtained with this ligand.^{7–9} Dicyanamide may act as a bidentate bridging ligand by coordinating to two different metal centres through its two terminal N(nitrile) atoms, or as a tridentate bridging ligand with additional coordination through the middle N(amide) atom (Scheme 1).^{10,11} Bidentate bridging coordination has been obtained in a few low-dimensional complexes with formula $[\text{ML}(\text{dca})_2]$ where L = unidentate ligand. Magnetic interactions reported to date are generally low, but the different kinds of interactions observed for Co(II) and Mn(II) are still not clear and deserve the attention of magnetochemists.

To continue the study of multinuclear dicyanamide bridged metal complexes we report here the synthesis and magnetic behaviour of two new Mn(II) compounds, $[\text{Mn}(\text{dca})_2(4\text{CN-py})_2]_n$ (**1**) and $[\text{Mn}(\text{dca})_2(\text{bpe})]_n$ (**2**). Compound **1** is a two-dimensional network with single end-to-end dca bridges whereas compound **2** is an one-dimensional chain with double end-to-end dca bridges.



Scheme 1

Experimental

General

$\text{NaN}(\text{CN})_2$, $\text{MnCl}_2 \cdot 4\text{H}_2\text{O}$ and 1,2-bis(4-pyridyl)ethane were purchased from Aldrich Chemical Company Inc., 4-cyanopyridine was purchased from E Merck and used as received. All other chemicals used were AR grade.

Elemental analyses (C, H, N) were performed using a Perkin–Elmer 240 elemental analyser. Magnetic susceptibility measurements were carried out for compounds **1** and **2** on polycrystalline samples with a SQUID magnetometer working in the range 2–300 K under a magnetic field of 0.05 T. Diamagnetic corrections were estimated from Pascal tables.¹² EPR spectra were recorded with a Bruker ES200 spectrometer at X-band frequency.

Syntheses

$[\text{Mn}(\text{dca})_2(4\text{CN-py})_2]_n$ (1**).** Compound **1** was synthesised by adding 1 mmol of 4-cyanopyridine to a solution of 1 mmol $\text{MnCl}_2 \cdot 4\text{H}_2\text{O}$ in 20 ml methanol, followed by addition of 2 mmol of sodium dicyanamide in 10 ml water. After filtering, the clear colourless filtrate was kept in a refrigerator. Colourless single crystals suitable for X-ray diffraction were obtained after a few days. Yield 60%. Anal. found (calcd.) for $\text{C}_{16}\text{H}_8\text{MnN}_{10}$ ($M = 395.26$): C, 48.43 (48.57); H, 1.90 (2.02); N, 35.10 (35.41).

$[\text{Mn}(\text{dca})_2(\text{bpe})]_n$ (2**).** Compound **2** was synthesised by adding 1 mmol of 1,2-bis(4-pyridyl)ethane to a solution of 1 mmol $\text{MnCl}_2 \cdot 4\text{H}_2\text{O}$ in 20 ml methanol, followed by addition of 2 mmol of sodium dicyanamide in 10 ml water. After filtering, the clear colourless filtrate was kept in a refrigerator. Colourless single crystals suitable for X-ray diffraction were obtained after a few days. Yield 60%. Anal. found (calcd.) for

Table 1 Crystal data and details of structure determination for complexes **1** and **2**

| Compound | 1 | 2 |
|---|---|---|
| Empirical formula | C ₁₆ H ₈ Mn N ₁₀ | C ₁₆ H ₁₂ Mn N ₈ |
| FW | 395.26 | 371.28 |
| T/K | 293 | 293 |
| Crystal system | Orthorhombic | Monoclinic |
| Space group | <i>Pccn</i> | <i>I 2/a</i> |
| <i>a</i> /Å | 9.479(4) | 13.078(4) |
| <i>b</i> /Å | 12.308(5) | 9.695(3) |
| <i>c</i> /Å | 14.402(5) | 14.592(5) |
| β /° | 90 | 105.74 |
| <i>u</i> /Å ³ | 1680.2(11) | 1780.7(10) |
| <i>Z</i> | 4 | 4 |
| μ /mm ⁻¹ | 0.811 | 0.757 |
| Reflect. collected | 4276 | 4297 |
| Unique reflect. | 2179 | 2214 |
| Obs. reflect. [<i>I</i> > 2 σ (<i>I</i>)] | 1801 | 1712 |
| <i>R</i> ^a | 0.0383 | 0.0409 |
| <i>wR</i> ₂ ^b | 0.1120 | 0.1106 |
| <i>R</i> (int) | 0.024 | 0.0288 |

^a $R = \sum ||F_o| - |F_c|| / \sum |F_o|$; ^b $wR = [\sum \{w(F_o^2 - F_c^2)^2\} / \sum \{w(F_o^2)^2\}]^{1/2}$

C₁₆H₁₂MnN₈ (*M* = 371.28): C, 51.92 (51.71); H, 2.97 (3.23); N, 30.00 (30.16).

Crystal structure determination

Data collections were carried out at 293(3) K, on a Nonius DIP-1030H system with Mo-K α radiation. A total of 30 frames were collected, each with an exposure time of 12 min, over a half of reciprocal space with a rotation of 6° about φ , the detector being at a distance of 90 mm from the crystal. Data reduction and cell refinement were carried out using the program Mosflm.¹³ The structures were solved by Patterson and Fourier analyses¹⁴ and refined by the full-matrix least-squares method based on F^2 with all observed reflections.¹⁵ All the calculations were performed using the WinGX System, ver. 1.64.¹⁶ Crystal data and refinement details of complexes **1** and **2** are given in Table 1.

CCDC reference numbers 190860 and 190861. See <http://www.rsc.org/suppdata/nj/b2/b202431b/> for crystallographic files in CIF or other electronic format.

Results and discussion

Crystal structures

[Mn(dca)₂(4CN-py)₂]_n (1). The manganese centre lies on a twofold axis in a distorted octahedral geometry, where four coordination sites are occupied by the nitrile groups of the anions and two *cis* positions by the 4CN-py ligands bound through the heterocycle nitrogen (Fig. 1). The latter Mn–N(py) distances of 2.345(2) Å are significantly longer than the former ones [2.203(2), 2.204(2) Å]. An analogous trend in the coordination sphere distances was observed in the 1D chains of Mn[N(CN)₂]₂(2,2'-bipym)(H₂O) (bipym = 2,2'-bipyrimidine),¹⁷ where the Mn–N(bipym) distances are 2.278(3) Å and those involving N(CN)₂[−] are 2.147(5) and 2.196(6) Å, for a bridging and terminal anion, respectively. The crystal structure consists of 2D rhomboid grid sheets, where the knots are occupied by the Mn(4CN-py)₂ units and the edges by the bridging dicyanamide ligands, with 4CN-py ligands that branch off from the 2D arrangement (Fig. 2). The layer is folded in a highly wavy fashion, as displayed in Fig. 3. The metal-metal distance inside the grid is 8.286 Å, and the Mn···Mn···Mn parallelogram angles are 95.92° and 69.77°. On the other hand, the nearest interlayer distance, of

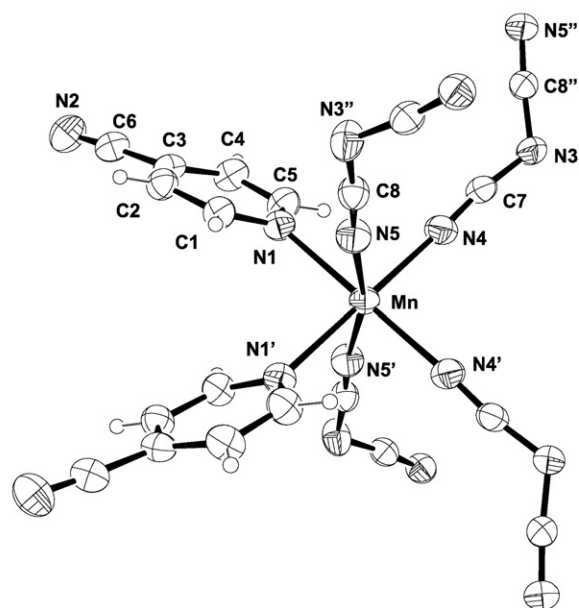


Fig. 1 ORTEP diagram (40% thermal ellipsoids) with atom labeling scheme of complex **1** [symmetry codes: (') $-x + 3/2, -y - 1/2, z$; (") $x - 1/2, -y, -z - 1/2$].

7.201 Å, is shorter due to the interdigitation of the 4CN-py groups (Fig. 3). This arrangement leads to the pyridine rings belonging to different sheets to stack at about 3.6 Å. The pyridine nitrile group is slanted with respect to the ring plane as defined by the N2–C6···N1 angle of 172.5(2)°. Selected bond lengths and angles are given in Table 2.

[Mn(dca)₂(bpe)]_n (2). The structure of compound **2** consists of linear 1D chains (Fig. 4) with metals connected by two bridging dicyanamides and by a bpe ligand. The manganese ion is located on a centre of symmetry and exhibits coordination bond angles that do not exceed 0.6° from the ideal octahedral geometry. The Mn–N distances with anion nitrile groups are 2.222(2) and 2.225(2) Å, those with the pyridine N donor are slightly longer, 2.267(2) Å. The conformationally flexible bpe adopts a *gauche* conformation with a C–C ethane bond torsion angle of 47.8(5)° and a dihedral angle of 62.52(5)° between the pyridyl rings. The Mn···Mn distance spanned by the bridging

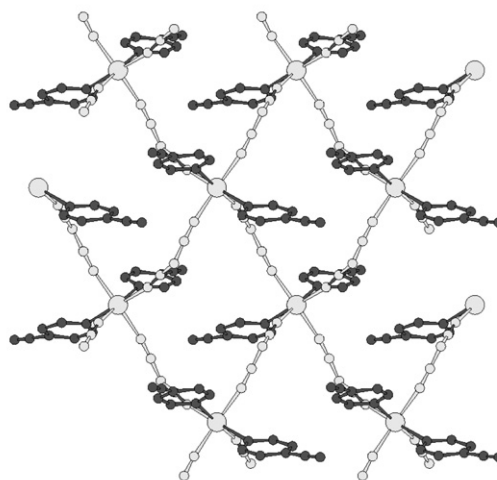


Fig. 2 View down crystallographic axis *c* of the 2D coordination rhomboid-grid sheet of complex **1** (the 4-CNpy atoms are shown in black).

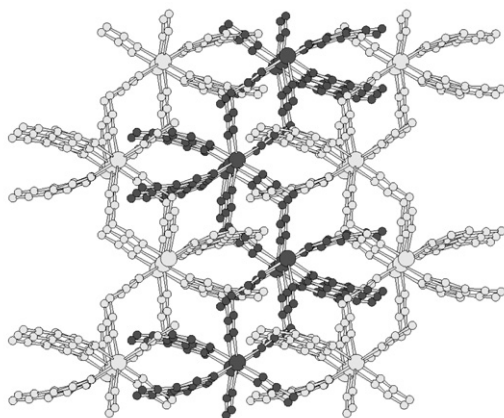


Fig. 3 Molecular packing of complex **1** along axis *a*, showing the interdigitation of 4CN-py ligands into adjacent parallelogram grid units.

ligands is 7.296 Å, while the closest interchain distance is 8.140 Å. Crystal packing shows bpe pyridine rings of different coordination polymers stacking at 4.2 Å. As comparison, intra-chain Mn...Mn distances of 14.045 Å and 13.993 Å were measured in the [Mn(bpe)(H₂O)₄]_n¹⁸ and [Mn(bpe)(-H₂O)₄]_{0.5n}-(bpe)_n polymers,¹⁹ respectively, where the bridging bpe presents an *anti* conformation. Selected bond lengths and angles are cited in Table 3.

Magnetic properties

The magnetic characterisation of complexes **1** and **2** was carried out through measurements of the variation of the magnetic susceptibility, χ_M , with temperature and the variation of the molar magnetisation with the field, at 2 K. The experimental data, plotted as the thermal variation of the susceptibility χ_M and the product $\chi_M T$ are shown in Fig. 5 for compound **1** and in Fig. 6 for compound **2**. The overall behaviour of **1** and **2** corresponds to weak antiferromagnetically coupled systems. The χ_M values continuously increase upon cooling, whereas $\chi_M T$ decreases slowly from 300 K down to 50 K, then more rapidly down to 2 K, tending to zero. The values of $\chi_M T$ at room temperature are 4.45 and 4.36 cm³ mol⁻¹ K for **1** and **2**, respectively, as expected for quasi-isolated $S = 5/2$ ions. This is in agreement with slight antiferromagnetic interactions in the compounds.

The susceptibility data of complex **1** have been fitted (Fig. 5) by means of the analytical expression derived by Curély²⁰ for an infinite 2D square lattice composed of classical spins ($S = 5/2$) isotropically coupled and based on the exchange Hamiltonian $H = -\sum_{mn} J_{ij} S_i S_j$ where S_{mn} runs over all pairs of nearest-neighbour spins i and j (Heisenberg couplings).^{20a,c}

$$\chi = [Ng^2\beta^2 S(S+1)(1+u)^2]/[3kT(1-u)^2] \quad (1)$$

Table 2 Selected bond distances (Å) and angles (°) in complex **1**^a

| | | | |
|---------------|-----------|---------------|-----------|
| Mn–N(1) | 2.345(2) | Mn–N(4) | 2.203(2) |
| Mn–N(5) | 2.204(2) | N(4)–C(7) | 1.154(2) |
| N(5)–C(8) | 1.153(2) | | |
| N(4)–Mn–N(1') | 179.94(6) | N(4)–Mn–N(1) | 86.69(6) |
| N(4)–Mn–N(4') | 93.28(8) | N(4)–Mn–N(5') | 95.02(6) |
| N(4)–Mn–N(5) | 94.60(6) | N(5')–Mn–N(5) | 165.97(9) |
| N(5)–Mn–N(1') | 85.45(6) | N(5)–Mn–N(1) | 84.94(6) |
| N(1')–Mn–N(1) | 93.33(8) | | |

^a Symmetry codes: (') $-x+3/2, -y-1/2, z$; (") $-x+1/2, -y+1/2, -z+3/2$.

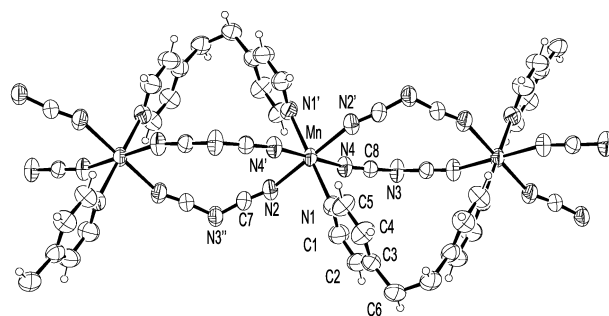


Fig. 4 Fragment of the chain (ORTEP diagram, 40% thermal ellipsoids) with atom labeling of complex **2** [symmetry codes: (') $\frac{1}{2} - x, \frac{1}{2} - y, \frac{3}{2} - z$; (") $x, \frac{1}{2} - y, \frac{1}{2} + z$].

where N is Avogadro's number, β Bohr's magneton, k Boltzmann's constant, and u is the well known Langevin function:

$$u = L[JS(S+1)/kT] = \coth[JS(S+1)/kT] - kT/JS(S+1) \quad (2)$$

The best fit leads to $J = -(0.154 \pm 0.001)$ cm⁻¹; $g = 2.010 \pm 0.001$. The agreement factor $R = \Sigma(\chi_M T_{\text{obs}} - \chi_M T_{\text{calc}})^2 / \Sigma(\chi_M T_{\text{calc}})^2$ is 1.46×10^{-4} which corresponds to an excellent experiment-theory agreement. We have verified the J value using the expansion series of Lines²¹ for an $S = 5/2$ antiferromagnetic quadratic layer:

$$Ng^2\beta^2/\chi|J| = 3\theta + (\Sigma C_n/\theta^{n-1}) \quad (3)$$

where $\theta = kT/|J|S(S+1)$; $C_1 = 4$; $C_2 = 1.448$, $C_3 = 0.228$, $C_4 = 0.262$, $C_5 = 0.119$, $C_6 = 0.017$. We have found $J = -0.17$ cm⁻¹, which is very close to the J which previously derived.

The interpretation of the susceptibility behaviour is very simple. When the temperature is being reduced the susceptibility increases as expected. This is due to the fact that there are more and more spins that are correlated in the lattice. Thus, starting from the paramagnetic regime at high temperature, the susceptibility becomes maximum when 2D ordering occurs. Curély has shown that, in the case upon which we focus and by differentiating eqn. (1), one has the numerical relationship:^{20d}

$$kT(\chi_{\text{max}}) = 1.2625 JS(S+1) \quad (4)$$

where J is expressed in Kelvins (K) whereas from Lines work²¹ one has:

$$kT(\chi_{\text{max}})_L = J[1.12 S(S+1) + 0.10] \quad (5)$$

which leads to an estimate of $kT(\chi_{\text{max}})$ with an uncertainty of 5%. Using the respective J values previously found, one derives from eqn. (4) $T(\chi_{\text{max}}) = 2.45$ K and from eqn. (5) $T(\chi_{\text{max}})_L = 2.42 \pm 0.12$ K; these values are both very close and lie at the border of the accessible temperature domain where the susceptibility shows a broad maximum. Thus, in our case, the susceptibility seems to diverge but, in reality, it

Table 3 Selected bond distances (Å) and angles (°) in complex **2**^a

| | | | |
|----------------|----------|----------------|----------|
| Mn–N(1) | 2.267(2) | Mn–N(2) | 2.225(2) |
| Mn–N(4) | 2.222(2) | N(2)–C(7) | 1.137(3) |
| N(4)–C(8) | 1.146(3) | | |
| N(4)–Mn–N(2) | 90.54(9) | N(4)–Mn–N(2') | 89.46(4) |
| N(4)–Mn–N(1) | 89.41(8) | N(4)–Mn–N(1') | 90.59(8) |
| N(2)–Mn–N(1'') | 90.47(9) | N(2)–Mn–N(1) | 89.53(9) |
| N(1)–Mn–N(1'') | 180.0 | N(4'')–Mn–N(4) | 180.0 |
| N(2'')–Mn–N(2) | 180.0 | | |

^a Symmetry codes: (') $-x+3/2, -y-1/2, z$; (") $-x+1/2, -y+1/2, -z+3/2$.

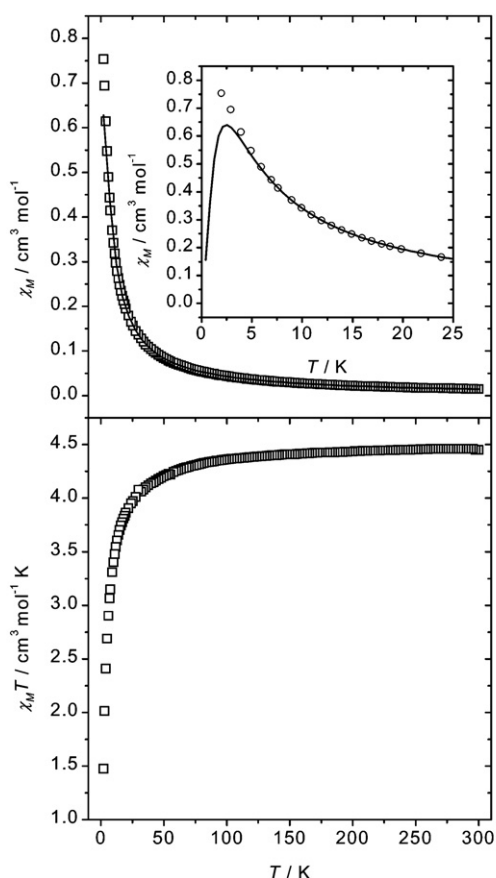


Fig. 5 Temperature dependence of χ_M (top) and $\chi_M T$ (bottom) for complex **1** with solid line showing the best fit obtained through χ_M values. Inset: low temperature region of χ_M . The solid line represents the simulation from 25 K to 0 K of the Curély expression with the coupling parameters given in the text. The χ_M value would tend to 0 cm³ mol⁻¹.

tends towards its maximum value (closer and closer to absolute zero when J is weaker and weaker) before decreasing and vanishing at 0 K, as expected for a compensated 2D isotropic antiferromagnet. Note that, from the experimental knowledge of $T(\chi_{\max})$, one can directly obtain the J value.

The weak value of the exchange energy characterising the antiferromagnetic coupling is also shown through the curve of $M/N\beta$ (reduced magnetization) vs. H (at 2 K), which always

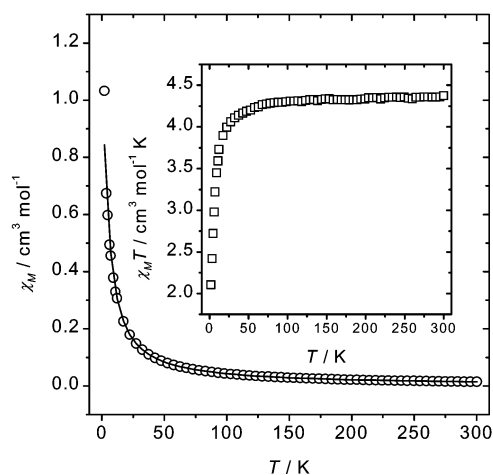


Fig. 6 Temperature dependence of χ_M for complex **2** with solid line showing the best fit obtained. Inset: plot of $\chi_M T$ vs. T data.

does not show any change of slope, thus proving the 2D magnetic behaviour at the lowest experimentally accessible temperature (Fig. 7). In addition, this curve of reduced magnetisation does not follow the Brillouin formula for an isolated $S = 5/2$ ion. The experimental data are situated below the theoretical curve, indicating a weak antiferromagnetic coupling. Indeed, this coupling must be very small, because at 5 Tesla, the $M/N\beta$ value tends to 4.5 (close to the theoretical value of 5.0, assuming $g = 2.00$).

The magnetic behaviour of compound **2** has been analysed by means of the analytical expression²² for an infinite chain of classical spins, scaled to $S = 5/2$, derived by Fisher :

$$\chi = [Ng^2\beta^2 S(S+1)(1+u)]/[3kT(1-u)] \quad (6)$$

where N , β , k and u have been defined above. The best fit leads to $J = -1.25$ cm⁻¹; $g = 2.00$. The agreement factor R was 2.2×10^{-4} , which also corresponds to an excellent experiment-theory agreement.

As for compound **1**, the weak antiferromagnetic coupling for compound **2**, is also shown through the curve of $M/N\beta$ (reduced magnetisation) vs. H (at 2 K), which does not show any change of slope, thus proving the 1D magnetic behaviour at the lowest experimentally accessible temperature. This curve of reduced magnetisation does not follow the Brillouin formula for an isolated $S = 5/2$ ion. Here also, the experimental data are situated below the theoretical curve, indicating weak antiferromagnetism. This coupling must be very small, because at 5 Tesla, the $M/N\beta$ value tends to 4.5 (close to the theoretical value of 5.0, assuming $g = 2.00$).

Considering the structural features for complexes **1** and **2**, the observed J values can be explained on the basis of the possible exchange pathways present in these compounds. In **1** each Mn(II) ion is surrounded by four dicyanamide bridges in the quadratic layer. Here two manganese ions are bridged by one dicyanamide ion, whereas in **2** there are two dicyanamide and one 1,2-bis(4-pyridyl)ethane bridges between two manganese ions. Assuming that the coupling through 1,2-bis(4-pyridyl)ethane is zero, the small J value could be attributed to the dicyanamide ions. The very weak coupling parameters in both **1** and **2** are due to the long length of the $\mu_{1,5}$ -dicyanamide superexchange pathway.²³ The calculated J parameter of **2** is slightly larger than that of **1**; this may be due to the double dicyanamide bridges in **2** whereas complex **1** is singly dicyanamide bridged. Moreover a somewhat shorter Mn-Mn distance in complex **2** compared to that in complex **1** also supports these observations.

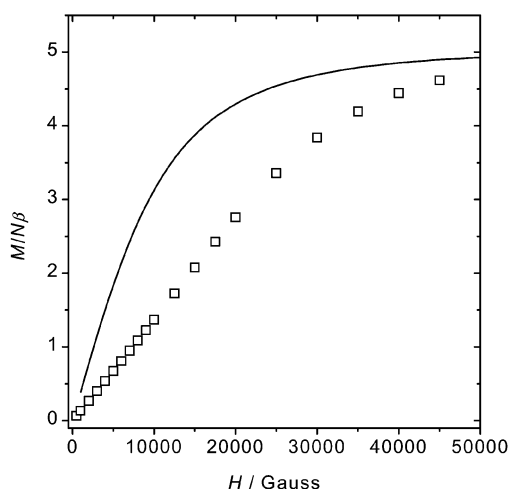


Fig. 7 Plot of reduced magnetisation vs. H data at 2 K for complex **1** revealing that the reduced magnetisation data do not follow the Brillouin formula for an isolated $S = 5/2$ ion.

The ESR spectra of complexes **1** and **2** allow one to determine that the spin-spin couplings are isotropic, with $g = 2.00$, as expected for Mn(II) ions. The bandwidth increases when the temperature decreases. This is due to the effect of dipolar interactions, as pointed out by Bencini and Gatteschi.²⁴

Conclusions

We presented here the syntheses, single crystal structures and low temperature magnetic behaviour of two new manganese(II) complexes **1** and **2** containing the dicyanamide ligand. Compound **1** is a 2D network consisting of octahedrally coordinated Mn(II) cations bridged by dicyanamide along with two monodentate 4-cyanopyridine ligands. Compound **2** is a 1D chain composed of octahedrally coordinated Mn(II), bridged by two dicyanamides as well as 1,2-bis(4-pyridyl)ethane. Fitting of the temperature dependent susceptibility data for complex **1** using the expansion series of Lines for an $S = 5/2$ antiferromagnetic quadratic layer, based on the exchange Hamiltonian, and for complex **2**, by the expression derived by Fisher for an infinite chain of classical spins, scaled to $S = 5/2$, reveals the existence of weak antiferromagnetic interactions in both complexes ($J = -0.154 \text{ cm}^{-1}$, $g = 2.01$ and $R = 1.46 \times 10^{-4}$ for **1** and $J = -1.25 \text{ cm}^{-1}$, $g = 2.00$ and $R = 2.2 \times 10^{-4}$ for **2**).

Acknowledgements

The authors sincerely thank Prof. J. Curély for taking part in scientific discussions. They also thank the Council of Scientific and Industrial Research (New Delhi) for funding (N.R.C).

References

- 1 P. S. Mukherjee, S. Dalai, E. Zangrando, F. Lloret and N. Ray Chaudhuri, *Chem. Commun.*, 2001, 1444.
- 2 T. K. Maji, P. S. Mukherjee, G. Mostafa, T. Mallah, J. C. Boquero and N. Ray Chaudhuri, *Chem. Commun.*, 2001, 1012.
- 3 P. S. Mukherjee, S. Dalai, G. Mostafa, T. H. Lu, E. Rentschler and N. Ray Chaudhuri, *New J. Chem.*, 2001, **25**, 1203.
- 4 P. S. Mukherjee, T. K. Maji, G. Mostafa, T. Mallah and N. Ray Chaudhuri, *Inorg. Chem.*, 2000, **39**, 5147.
- 5 P. S. Mukherjee, T. K. Maji, G. Mostafa, J. Ribas, M. S. El Fallah and N. Ray Chaudhuri, *Inorg. Chem.*, 2001, **40**, 928.
- 6 P. S. Mukherjee, S. Dalai, G. Mostafa, E. Zangrando, T. H. Lu, G. Rogez, T. Mallah and N. Ray Chaudhuri, *Chem. Commun.*, 2001, 1346.
- 7 I. Dasna, S. Golhen, L. Ouahab, N. Daro and J. P. Sutter, *New J. Chem.*, 2001, **25**, 1572.
- 8 (a) S. R. Batten, P. Jensen, B. Moubaraki, K. S. Murray and R. Robson, *Chem. Commun.*, 1998, 439; (b) M. Kurmoo and C. J. Kepert, *New J. Chem.*, 1998, **22**, 1515.
- 9 P. Jensen, S. R. Batten, B. Moubaraki and K. S. Murray, *Chem. Commun.*, 2000, 793.
- 10 (a) Y. M. Chow, *Inorg. Chem.*, 1971, **10**, 1938; (b) Y. M. Chow and D. Britton, *Acta Crystallogr. Sect. C*, 1977, **697**, 33.
- 11 J. L. Manson, C. R. Kmety, Q. Haung, J. W. Lynn, G. Bendele, S. Pagola, P. W. Stephens, L. M. Liable-Sands, A. L. Rheingold, A. Epstein and J. S. Miller, *Chem. Mater.*, 1998, **10**, 2552.
- 12 O. Kahn, *Molecular Magnetism*, VCH, Weinheim, 1993.
- 13 Collaborative Computational Project Number 4, *Acta Crystallogr. Sect. D*, 1994, **50**, 760.
- 14 G. M. Sheldrick, *Acta Crystallogr. Sect. A*, 1990, **46**, 467.
- 15 G. M. Sheldrick, SHELXS-97, Program for Crystal Structure Refinement, University of Göttingen, Germany, 1997.
- 16 L. J. Farrugia, WinGX-A Windows Program for Crystal Structure Analysis, University of Glasgow, Glasgow, 1998.
- 17 S. R. Marshall, C. D. Incarvito, J. L. Manson, A. L. Rheingold and J. S. Miller, *Inorg. Chem.*, 2000, **39**, 1969.
- 18 C. S. Hong, S.-K. Son, Y. S. Lee, M.-J. Jun and Y. Do, *Inorg. Chem.*, 1999, **38**, 5602.
- 19 C. S. Hong and Y. Do, *Inorg. Chem.*, 1998, **37**, 4470.
- 20 (a) J. Curély, *Europhys. Lett.*, 1995, **32**, 529; (b) J. Curély, *Physica B*, 1998, **254**, 263; (c) J. Curély, *Physica B*, 1998, **254**, 277; (d) J. Curély and J. Rouch, *Physica B*, 1998, **254**, 298.
- 21 M. E. Lines, *J. Phys. Chem. Solids*, 1970, **31**, 101.
- 22 M. E. Fisher, *Am. J. Phys.*, 1964, **32**, 343.
- 23 (a) S. Martin, M. G. Barandika, J. I. Ruiz de Larramendi, R. Cortés, M. Font-Bardía, L. Lezama, Z. E. Serna, X. Solans and T. Rojo, *Inorg. Chem.*, 2001, **40**, 3687, and references therein; (b) M. L. Manson, C. D. Incarvito, A. L. Rheingold and J. S. Miller, *J. Chem. Soc., Dalton Trans.*, 1998, 3705; (c) B.-W. Sung, S. Gao, B.-Q. Ma, D.-Z. Niu and Z.-M. Wang, *J. Chem. Soc., Dalton Trans.*, 2000, 4187; (d) P. Jensen, D. J. Price, S. R. Batten, B. Moubaraki and K. S. Murray, *Chem. Eur. J.*, 2000, **6**, 3186.
- 24 A. Bencini, D. Gatteschi, *EPR of Exchange Coupled Systems*, Springer-Verlag, Berlin, 1990.